MALAYSIAN JOURNAL OF MICROSCOPY

Journal homepage: https://malaysianjournalofmicroscopy.org

RESEARCH ARTICLE

STRUCTURAL AND COMPOSITIONAL EFFECTS OF CELLULOSE NANOFIBER–GRAPHENE/BI_2TE_3 NANOCOMPOSITE FILMS FABRICATED BY ELECTRODEPOSITION

Muhd Aliff Ikhwan Che Azman[1], Khairul Fadzli Samat[1,*], Nik Ahmad Luqman Hakim Nik AbdulRashid[1], Muhd Afiff Alias[1], Rose Farahiyan Munawar[1], Takahito Ono[2]

[1]*Faculty of Industrial and Manufacturing Technology and Engineering, Universiti Teknikal Malaysia Melaka, Durian Tunggal, Melaka, Malaysia.*

[2]*Department of Mechanical Systems Engineering, Tohoku University, Sendai, Japan.*

Abstract. Cellulose nanofiber (CNF) is a naturally derived nanomaterial known for its low thermal conductivity, making it an eco-friendly candidate for thermoelectric applications. This study explores the development of a CNF–graphene/Bi_2Te_3 nanocomposite thermoelectric material fabricated via electrodeposition using a three-electrode potentiostat setup. Electrolyte solutions containing nitric acid, bismuth-telluride ions, graphene, and varying CNF concentrations (0.5–2.0 g/L) were prepared to investigate CNF incorporation. The resulting films exhibited uniform distribution of CNF and graphene, with CNF content reaching up to 7.17 wt%. The Bi/Te atomic ratio remained stable (within 3.0% of the stoichiometric Bi_2Te_3 phase), and the average grain size was reduced by ~35% compared to pristine Bi_2Te_3, enhancing phonon scattering and electron mobility. X-ray diffraction (XRD) confirmed the rhombohedral Bi_2Te_3 (R3-m) structure with characteristic (1010), (015), and (110) peaks. No CNF or graphene peaks were detected, indicating successful incorporation without the formation of separate crystalline phases. Increasing CNF content reduced and broadened the (1010) peak, with crystallite size decreasing from 32.2 nm to 21.3 nm (CNF–III). A slight shift toward higher 2θ in CNF–III suggests interfacial strain and hybrid structural interactions. These structural modifications—grain refinement, disrupted long-range crystallinity, and interfacial effects—are expected to enhance thermoelectric performance by reducing lattice thermal conductivity and improving charge transport. The CNF–graphene/Bi_2Te_3 hybrid film thus demonstrates strong potential for next-generation thermoelectric materials.

Keywords: Thermoelectric film, electrodeposition, cellulose nanofiber.

Article Info

Received 5 March 2025
Accepted 18 October 2025
Published 4 December 2025

***Corresponding author: khairul.fadzli@utem.edu.my**

ISSN: 1823-7010, eISSN: 2600-7444

1. INTRODUCTION

Thermoelectric generators (TEGs) are a very promising technology for sustainable energy harvesting, as they enable the direct conversion of heat energy into electrical energy via the Seebeck effect. In this phenomenon, a temperature gradient across a material drives charge carriers (electrons or holes) from the hot side to the cold side, producing an electric potential. [1]. With increasing global energy demands and the urgent need for sustainable solutions, TEGs offer an effective method for harnessing waste heat from diverse sources, including industrial processes, automotive exhaust, and ambient environmental heat. The thermoelectric (TE) material in a TEG device is crucial for enhancing its efficiency. The performance of a TE material is evaluated using its figure of merit (*ZT*), where a high *ZT* value indicates an optimal combination of high electrical conductivity (σ), low thermal conductivity (κ), and a high Seebeck coefficient (S) [2,3]. Bismuth telluride (Bi_2Te_3) remains the leading TE material for room- and low-temperature applications due to its favorable electrical properties, large effective mass, and inherently low thermal conductivity. Bulk Bi_2Te_3 can reach ZT values of up to 0.7. However, pristine Bi_2Te_3 films synthesized by electrochemical deposition typically exhibit significantly lower performance, with ZT values dropping to 0.02 [4-6]. Despite this limitation, electrochemical deposition remains attractive due to its cost-effectiveness and compatibility with microfabrication for the fabrication of miniaturized devices [7]. To overcome the poor film performance, various approaches have been explored, including nano structuring, doping, and nanocomposite formation [8]. Nanocomposites, in particular, offer significant advantages by simultaneously tailoring electronic and thermal transport while improving mechanical strength.

In line with Jianghan et al. [9], demonstrated that incorporating cellulose nanofiber (CNF) into Bi_2Te_3-based thermoelectric films notably decreased thermal conductivity, achieving a value as low as 0.35 W mK^{-1} at an optimal concentration of 0.06 wt.%, which facilitated better thermoelectric performance by maintaining high temperature gradients. This microstructural engineering, along with phonon scattering, contributed to an impressive enhancement of the ZT value by approximately 625%, from 0.124 in pure Bi_2Te_3 to 0.76. The combination of low thermal conductivity and improved electrical properties demonstrates that CNF is an effective additive for significantly boosting thermoelectric efficiency. Besides that, Alias et al.[10], emphasize that incorporating graphene into electrodeposited Bi_2Te_3 nanocomposite films results in smaller grain sizes and the formation of crystalline defects such as stacking faults and grain boundaries, which significantly enhance phonon scattering. These microstructural changes lead to a reduction in thermal conductivity while maintaining electrical conductivity, thereby potentially improving the overall thermoelectric efficiency of the material.

Cellulose nanofibers (CNF) and graphene represent promising additives to Bi_2Te_3-based nanocomposites. Graphene enhances charge carrier mobility, improving electrical conductivity, while CNF serves as a reinforcing phase that reduces thermal conductivity and improves mechanical integrity, including hardness and Young's modulus [11,12]. Despite these benefits, limited research has systematically studied the combined influence of CNF and graphene in electrodeposited Bi_2Te_3 films. This study addresses that gap by fabricating CNF–graphene/Bi_2Te_3 nanocomposite films via electrochemical deposition and examining their structural and morphological evolution. The co-inclusion of CNF and graphene leads to notable grain refinement, increased lattice strain, and a higher grain boundary density. These microstructural features are expected to enhance phonon scattering and suppress lattice thermal conductivity, while graphene establishes efficient electrical transport pathways and CNF strengthens mechanical resilience.

The primary focus of this work is to examine how varying CNF concentrations influence the structural evolution, crystallinity, grain size, lattice strain, and stoichiometry of CNF–graphene/Bi_2Te_3 nanocomposites. By systematically identifying the optimal CNF content that enables microstructural refinement without compromising electrical efficiency, this research proposes a scalable, sustainable, and mechanically robust strategy for advancing Bi_2Te_3-based films. Ultimately, the designed hybrid nanocomposites aim to accelerate the development of next-generation thermoelectric devices with enhanced performance and long-term reliability.

2. MATERIALS AND METHODS

In this study, an electrolyte solution containing 3.2 mM Bi^{3+} and 7.2 mM $HTeO_2^+$ in HNO_3 was prepared, with graphene and cellulose nanofiber (CNF) added at concentrations ranging from 0.5 to 2.0 g/L. The solution was periodically stirred and sonicated to achieve optimal dispersion and suspension of the nanomaterials. A nanocomposite film was synthesized by a potentiostatic electrochemical deposition system with a three-electrode cell at room temperature. The electrochemical cell consisted of a Platinum (Pt) mesh as the counter electrode (CE), a silver/silver chloride (Ag/AgCl) reference electrode (RE), and a chromium-gold (Cr-Au) seed layer on a glass substrate as the working electrode (WE). Electrodeposition was conducted via a pulse deposition method, where each cycle involved applying a potential E_{on} for a duration t_{on}, followed by an applied potential E_{off} for a duration t_{off}. Rapid co-deposition occurred during the 100 ms t_{on} at an applied potential of –90 mV, E_{on}, whereas no deposition was observed during the E_{off} period. Prior to deposition, the CNF was mixed and sonicated with poly (diallyldimethylammonium chloride) (PDDA) to ensure complete wrapping by the polymer molecules [13]. The CNF-PDDA mixture was then filtered to remove excess PDDA before being added to the electrolyte. The overall film fabrication process as shown in Figure 1. The surface morphology of CNF-Graphene/Bi_2Te_3 films was examined using field emission scanning electron microscopy (FESEM), while their elemental composition was analyzed with an energy-dispersive X-ray spectrometer (EDX) integrated into the FESEM. Crystal orientation and crystallite size were characterized through X-ray diffraction (XRD).

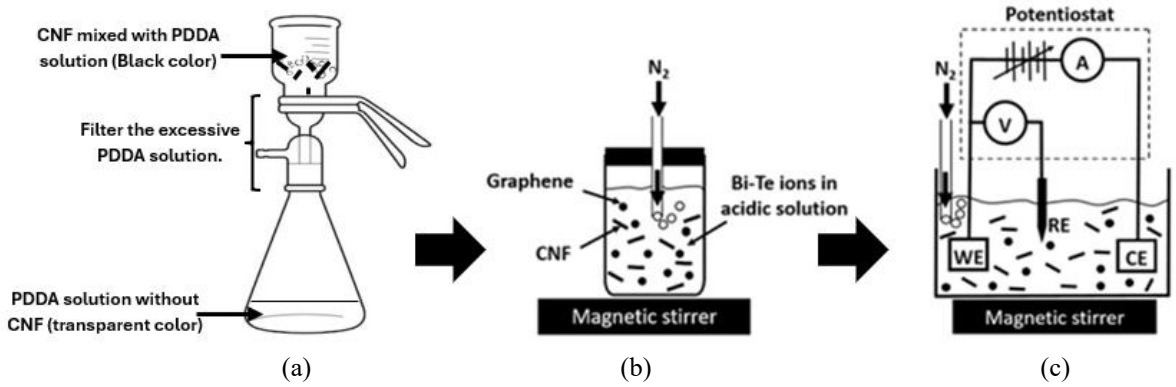

Figure 1: Overview of the film fabrication process incorporating Cellulose Nanofiber (CNF) and graphene: (a) filtration of CNF mixed with PDDA, (b) preparation of the electrolyte and (c) electro-codeposition process

3. RESULTS AND DISCUSSION

Figure 2 shows the cyclic voltammograms (CVs) of pristine Bi_2Te_3 and CNF (0.5)-Graphene/Bi_2Te_3. Cyclic voltammetry was performed on both samples to analyze the oxidation-reduction (redox) reaction at the working electrode and determine the optimal potential range for electrodeposition. The reduction peaks for pristine Bi_2Te and CNF (0.5)-Graphene/Bi_2Te were identified as R1 and R2, respectively. A significant shift (negatively) in the reduction peak was observed for CNF (0.5)-Graphene/Bi_2Te_3 compared to pristine Bi_2Te. This shift is attributed to the co-deposition of graphene and cellulose nanofiber (CNF) during Bi_2Te_3 reduction, which enhances electron transfer at the working electrode surface [10]. The reduction peak R2 was recorded at -100 mV, while R1 appeared at approximately -40 mV. A fixed potential of -90 mV (R2) was applied for all electrodepositions due to its role in promoting improved morphological growth of the deposited films in both CNF-Graphene/Bi_2Te_3 and pristine Bi_2Te_3 [14]. The use of a higher cathodic potential during the electrodeposition of CNF-Graphene/Bi_2Te_3 led to an increase in the reduction current. This indicates

that a greater number of electrons were transferred during the diffusion of Bi/Te ions. The positively charged surface of NMP-coated graphene nanoparticles and PDDA-coated with CNF can promote stable electrolytic co-deposition by attracting negatively charged ions from the electrolyte solution. This results in the formation of a stable suspension of graphene nanoparticles in the solution, which can then be co-deposited with other materials such as Bi^{3+} and $HTeO^{2+}$ during the electrodeposition process. The positively charged surface of the graphene nanoparticles is achieved through the adsorption of metal ions on their surface, resulting in a positive charge on the nanoparticle surface [15]. This positive charge can attract negatively charged ions from the electrolyte solution, leading to the formation of a stable suspension of graphene nanoparticles in the solution. The stable suspension can then be co-deposited with other materials, leading to the formation of a composite material with enhanced properties [16].

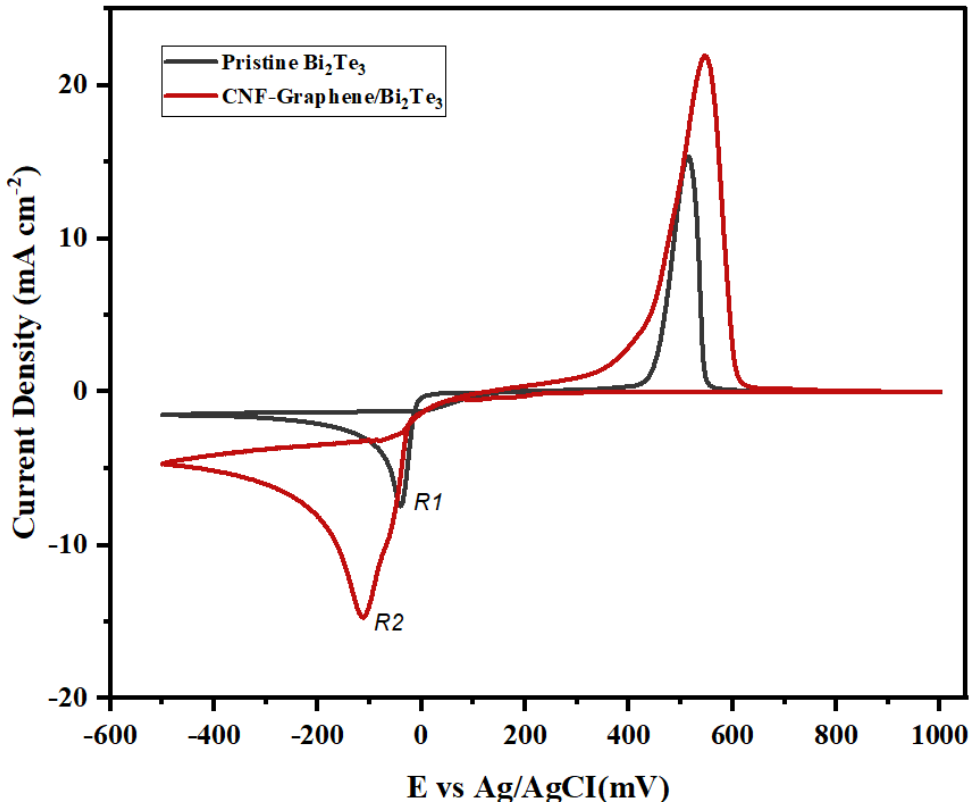

Figure 2 : Cyclic voltammograms of the pristine Bi_2Te_3 and CNF- Graphene/Bi_2Te_3

Table 1 summarizes the elemental composition of the deposited CNF-Graphene/Bi_2Te_3 nanocomposite films and the corresponding electrolytes used in the study. Five electrolyte solutions (I–V) were evaluated, differentiated by the amount of CNF incorporated. On average, the graphene content in the nanocomposite films remained consistent, with weight percentages showing no significant variation across all electrolytes. These included an electrolyte that did not include graphene and CNF, which was used to produce the pristine Bi_2Te_3 film. Another three electrolytes comprised of the inclusion of CNF up to 2 gL^{-1} in the electrolyte solution. Based on average values obtained from EDX measurements, the co-deposited CNF content in the nanocomposite film was evaluated as carbon weight percentage (C-wt.%). Up to 5.57% CNF has successfully been deposited in the nanocomposite film. There is a pattern where the CNF content starts from samples three to five and gradually increases. This indicates that as CNF increases in electrolytes, the carbon composition rate in the deposited film also increases. The incorporated CNF in the film was recorded by comparing the graphene/Bi_2Te_3 film. The Bi/Te atomic ratio remained consistent across varying CNF concentrations, with the atomic percentage error relative to the stoichiometric ratio of the Bi_2Te_3 phase consistently staying below 3%. Based on the ideal Bi_2Te_3 ratio (40:60), this error was deemed acceptable, staying within a margin of no more than 3%. It is recommended that the ratio fluctuation of Bi-Te should not exceed 5% error from the

pristine one. This is being done to prevent any potential ratio factor from affecting TE performance. The morphological analysis was conducted to study the microstructure of both pristine Bi_2Te_3 and CNF-graphene/Bi_2Te_3 films. The CNF-graphene inclusion affected the growth of the Bi2Te3 microstructure. Figure 3(a) displays a typical pristine Bi_2Te_3 microstructure, which is known as a plate-like or needle-like structure [17,18]. Figure 3(b) to (d) present the morphological images of nanocomposite films with varying CNF concentrations, clearly illustrating the co-deposition of CNF within the Bi_2Te_3 matrix. The random orientation of CNFs contributes to a finer microstructure with more grain boundaries. Each grain boundary serves as a scattering center for phonons, disrupting their coherent propagation and thereby reducing thermal conductivity [19].

Table 1: Element composition of electrodeposited film from EDX analysis

Electrolyte	Nanomaterial concentration in electrolyte (g/L)		Electrodeposited films	Composition in the deposited film		
	Graphene	Cellulose nanofiber (CNF)		Carbon (wt.%)	Bi: Te (at%)	Atomic percentage error due to Bi_2Te_3 phase ratio (%)
I	0.00	0.0	Bi_2Te_3	0.00	40:60	0
II	0.75	0.0	Bi_2Te_3/Graphene	1.60	37:63	±3
III	0.75	0.5	CNF-Graphene /Bi_2Te_3-I	3.95	42:58	±2
IV	0.75	1.0	CNF-Graphene /Bi_2Te_3-II	5.40	42:58	±2
V	0.75	2.0	CNF-Graphene /Bi_2Te_3-III	7.17	43:57	±3

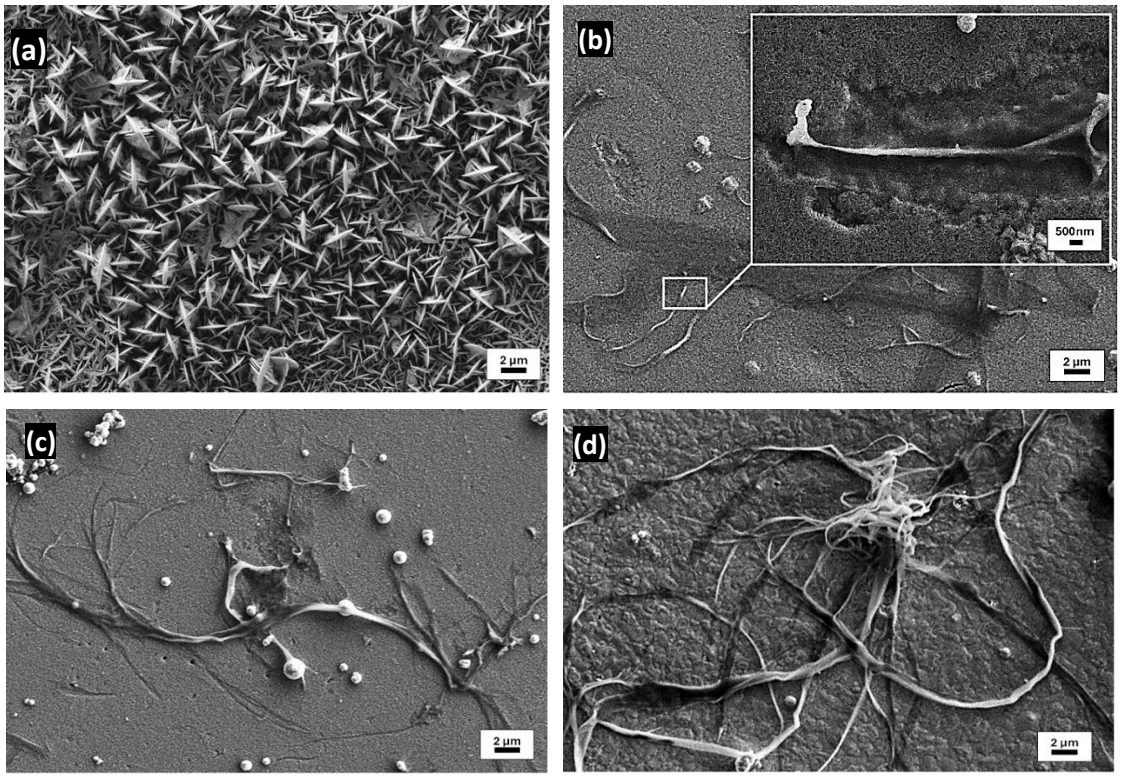

Figure 3: SEM images of electrodeposited film surface (a)Bi_2Te_3 (b) CNF-Graphene /Bi_2Te_3-I (c) CNF-Graphene /Bi_2Te_3-II and (d) CNF-Graphene /Bi_2Te_3-III

Figure 4 presents the XRD patterns of pristine Bi_2Te_3 and CNF–graphene/Bi_2Te_3 nanocomposite films with CNF concentration up to 7.17 wt.%. All films exhibit diffraction peaks characteristic of rhombohedral Bi_2Te_3 (R3-m), including the (1010), (015), and (110) planes, in agreement with previous reports on electrodeposited Bi_2Te_3 [20-23]. No additional peaks corresponding to CNF or graphene were detected, confirming that these inclusions were well incorporated into the Bi_2Te_3 matrix without forming separate crystalline phases. With increasing CNF concentration, the (1010) peak intensity decreased, and its width broadened, reflecting a reduction in crystallite size and an increase in lattice strain. Scherrer analysis showed that the average crystallite size decreased from 32.2 nm for pristine Bi_2Te_3 to 21.3 nm for the CNF-III nanocomposite, consistent with the microstrain values presented in Table 2. Furthermore, in the CNF–III sample, the (1010) peak exhibited a slight shift toward higher 2θ values, which can be attributed to several factors related to structural, compositional, and interfacial modifications within the nanocomposite film [24]. This shift suggests the presence of interfacial strain and hybrid structural interactions between Bi_2Te_3, CNFs, and graphene. These results indicate that the CNF and graphene inclusions promote grain refinement, disrupt long-range crystallinity, and generate hybrid interfacial effects, which are expected to enhance phonon scattering and reduce lattice thermal conductivity.

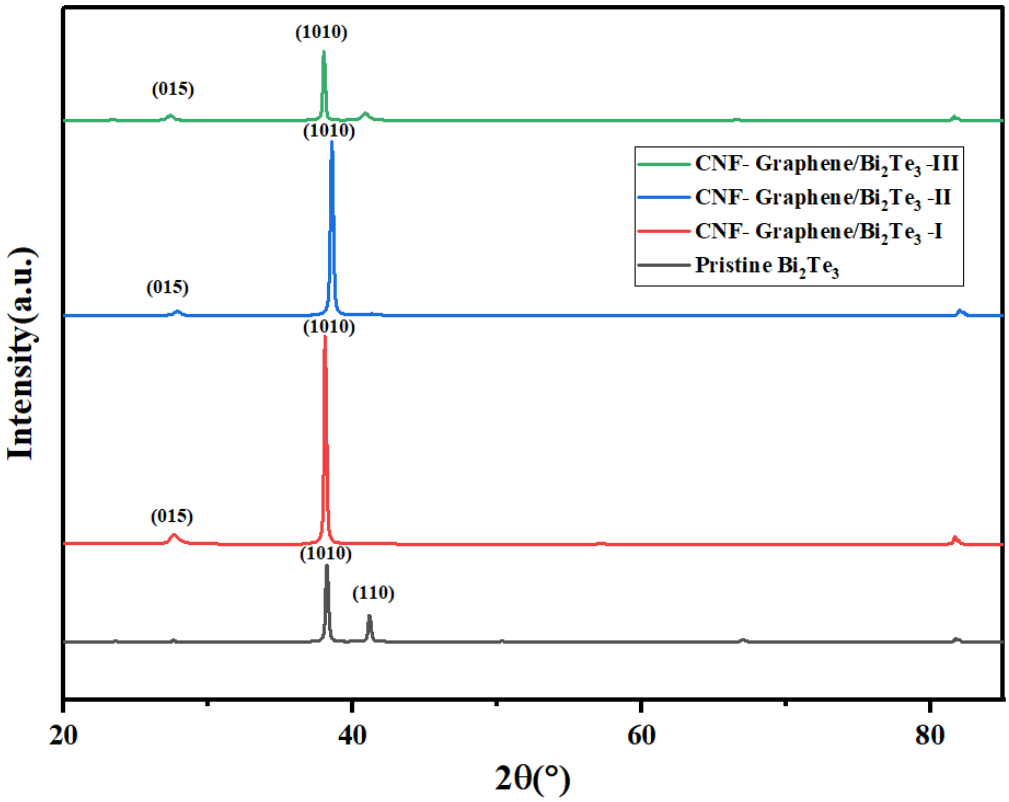

Figure 4: XRD results for electrodeposited film

The average grain size was determined using the Scherrer equation, utilizing the Full Width at Half Maximum (FWHM) and the integral breadth (β) of the Bi_2Te_3 peaks. In polycrystalline materials, the crystallite grain size is typically uniform in size and distribution, making it comparable to the grain size. As indicated in Table 2, the grain size decreased with the addition of higher amounts of CNF to the nanocomposite. The pure Bi_2Te_3 film exhibited the largest crystallite size, 32.20 ± 4.3 nm, while the inclusion of graphene reduced this size to 24.80 ± 1 nm [10], indicating a grain refinement effect. As CNF content increased, the crystallite size decreased, with the smallest grain size observed in the 5.57 wt% CNF film. The smallest grain size was calculated to be approximately 21.32 nm, representing a reduction of about 35% compared to the pure Bi_2Te_3 film. This reduction in grain size is known to significantly enhance the figure of merit (ZT) [25]. The average microstrain, a measure of lattice

distortion and internal stress, was 4.30×10^{-3} for the pure Bi_2Te_3 film. With the addition of CNF, the microstrain increased, peaking at 5.18×10^{-3} at 1.2 wt.% CNF, before slightly decreasing at higher CNF concentrations. This trend indicates that incorporating CNF introduces lattice strain, which is most pronounced at lower CNF concentrations but stabilizes as CNF content increases. The increased lattice strain enhances phonon scattering, further reducing thermal conductivity. Additionally, the smaller grain size increased the density of grain boundaries, enhancing phonon scattering caused by lattice misalignments at these boundaries and further disrupting the coherent transmission of heat [26].

Table 2: Summary of average crystallite grain size on the deposited film

Film type	Average crystallite grain size, D (nm)	Integral Breadth, L	Average Microstrain, ϵ (X 10^-3)
Bi_2Te_3	32.20 ± 4.3	0.60	4.30
Graphene/Bi_2Te_3 [10]	24.80 ± 1.0	0.56	_
CNF- Graphene /Bi_2Te_3.I	25.09± 1.2	0.24	5.18
CNF- Graphene /Bi_2Te_3-II	24.10 ± 1.2	0.26	4.92
CNF - Graphene /Bi_2Te_3-III	21.32 ± 1.4	0.31	5.13

4. CONCLUSIONS

This study successfully demonstrated the electrodeposition of CNF–graphene/Bi_2Te_3 nanocomposite films and evaluated the influence of CNF concentration on their microstructure and crystallinity. By varying CNF content in the electrolyte, films with up to 7.17 wt.% CNF were produced, achieving uniform incorporation of CNF and graphene within the Bi_2Te_3 matrix. X-ray diffraction (XRD) confirmed the preservation of the rhombohedral Bi_2Te_3 (R3-m) structure across all samples, with no detectable secondary phases from CNF or graphene. Increasing the CNF concentration led to a notable reduction in crystallite size, from 32.2 nm to 21.3 nm, along with peak broadening and a slight shift in the (1010) peak toward higher 2θ angles, indicating lattice strain and hybrid interfacial interactions. These structural modifications, including grain refinement, disrupted long-range crystallinity, and increased defect density (e.g., stacking faults and grain boundaries), are expected to enhance thermoelectric performance by promoting electron and phonon scattering. This, in turn, contributes to reduced lattice thermal conductivity and potentially improves the overall figure of merit (ZT). The findings reinforce the potential of CNF–graphene/Bi_2Te_3 hybrid films as promising candidates for next-generation, eco-friendly thermoelectric materials.

Acknowledgements

The authors would like to express their sincere gratitude to Universiti Teknikal Malaysia Melaka (UTeM) for all the support provided. This research is funded by Ministry of Higher Education (MOHE) of Malaysia through the Fundamental Research Grant Scheme (FRGS), No: FRGS/1/2023/ TK08/UTeM/02/5.

Author Contributions

All authors contributed toward data analysis, drafting and critically revising the paper and agree to be accountable for all aspects of the work.

Disclosure of Conflict of Interest

The authors have no disclosures to declare

Compliance with Ethical Standards

The work is compliant with ethical standards

References

[1] Yuan, D., Jiang, W., Sha, A., Xiao, J., Wu, W., & Wang, T. (2023). Technology method and functional characteristics of road thermoelectric generator system based on Seebeck effect. *Applied Energy*, *331*, 120459.

[2 Keshavarz, M. K., Vasilevskiy, D., Masut, R. A. & Turenne, S. (2016). Mechanical properties of bismuth telluride-based alloys with embedded MoS2 nanoparticles. *Materials and Design*, 103, 114–121.

[3] Rathi, V., Singh, K., Parmar, K. P. S., Brajpuriya, R. K. & Kumar, A. (2024). Boosting thermoelectric performance of PEDOT: PSS/Bi2Te3 hybrid films via structural and interfacial engineering. *Organic Electronics*, 133, 107103–107103.

[4] Mori, R., Mayuzumi, Y., Yamaguchi, M., Kobayashi, A., Seki, Y. & Takashiri, M. (2020). Improved thermoelectric properties of solvothermally synthesized Bi_2Te_3 nanoplate films with homogeneous interconnections using Bi_2Te_3 electrodeposited layers. *Journal of Alloys and Compounds*, 818, 152901.

[5] Toan, N., Kim Tuoi, T. T. K., Samat, K. F., Sui, H., Inomata, N., Toda, M. & Ono, T. (2020). High performance micro-thermoelectric generator based on metal-doped electrochemical deposition. In *Proceedings of the 33rd IEEE International Conference on Micro Electro Mechanical Systems (MEMS 2020)*, Vancouver, 18–22 January 2020.

[6] Norimasa, O. & Takashiri, M. (2021). In-and cross-plane thermoelectric properties of oriented Bi2Te3 thin films electrodeposited on an insulating substrate for thermoelectric applications. *Journal of Alloys and Compounds*, 899, 163317.

[7] Nguyen Huu, T., Nguyen Van, T. & Takahito, O. (2017). Flexible thermoelectric power generator with Y-type structure using electrochemical deposition process. *Applied Energy*, 210, 467–476.

[8] Samat, K. F., Trung, N. H. & Ono, T. (2019). Enhancement in thermoelectric performance of electrochemically deposited platinum-bismuth telluride nanocomposite. *Electrochimica Acta*, 312, 62–71.

[9] Jianghan, T., Toan, N. V., Keita, S., Kim Tuoi, T., Samat, K. F., Tran, N., van Hieu, N. & Ono, T. (2025). Enhanced thermoelectric performance of electrochemically deposited cellulose nanofiber-bismuth telluride nanocomposite. *Journal of the Electrochemical Society*, 172(4), 043501.

[10] Alias, M. A., Samat, K. F., Mohamad, N., Warikh, M. W. A., Azam, M. A., Toan, N. V., Ono, T., Klimkowicz, A. & Takasaki, A. (2023). Electrodeposited bismuth telluride nanocomposite thermoelectric film with improved graphene deposition. *Journal of Advanced Research in Applied Mechanics*, 111(1), 161–172.

[11] Zhao, X., Zhao, C., Jiang, Y., Ji, X., Kong, F., Lin, T., Shao, H. & Han, W. (2020). Flexible cellulose nanofiber/Bi_2Te_3 composite film for wearable thermoelectric devices. *Journal of Power Sources*, 479, 229044–229044.

[12] Ahmad, K., Wan, C., Al-Eshaikh, M. A. & Kadachi, A. N. (2019). Enhanced thermoelectric performance of Bi2Te3 based graphene nanocomposites. *Applied Surface Science*, 474, 2–8.

[13] Nurazzi, N. M., Rizal, M. R. M., Abdan, A., Abdullah, N., Sabaruddin, F. A., Kamarudin, S. H., Ahmad, S., Mahat, A. M., Lee, C. L., Aisyah, H. A., Norrrahim, M. N. F., Ilyas, R. A., Harussani, M. M., Ishak, M. R., Sapuan, S. M. (2021). Fabrication, functionalization, and application of carbon nanotube-reinforced polymer composite: an overview. *Polymers*, 13(7), 1047.

[14] Samat, K. F., Li, Y., Van Toan, N., Azam, M. A. & Ono, T. (2022). Highly enhanced thermoelectric and mechanical properties of Bi2Te3 hybrid nanocomposite with inclusion of Pt nanoparticles and SWCNTs. *Journal of Materials Research*, 37(20), 3445–3458.

[15] Ma, Y., Han, J., Wang, M., Chen, X. & Jia, S. (2018). Electrophoretic deposition of graphene-based materials: A review of materials and their applications. *Journal of Materiomics*, 4(2), 108-120.

[16] Samsudin, A. M., Roschger, M., Wolf, S. & Hacker, V. (2022). Preparation and characterization of QPVA/PDDA electrospun nanofiber anion exchange membranes for alkaline fuel cells. *Nanomaterials*, 12(22), 3965.

[17] Wang, W. -L., Wan, C. -C. & Wang, Y. -Y. (2007). Composition-dependent characterization and optimal control of electrodeposited Bi2Te3 films for thermoelectric application. *Electrochimica Acta*, 52(23), 6502–6508.

[18] Ma, Y., Ahlberg, E., Sun, Y., Iversen, B. B. & Palmqvist, A. E. C. (2011). Thermoelectric properties of thin films of bismuth telluride electrochemically deposited on stainless steel substrates. *Electrochimica Acta*, 56(11), 4216–4223.

[19] Hosseini, S. A., Romano, G. & Greaney, P. A. (2021). Mitigating the effect of nanoscale porosity on thermoelectric power factor of Si. *ACS Applied Energy Materials*, 4(2), 1915–1923.

[20] Li, S., Zhang, S., He, Z., Toprak, M., Stiewe, C., Muhammed, M. & Mueller, E. (2010). Novel solution route synthesis of low thermal conductivity nanocrystalline bismuth telluride. *Journal of Nanoscience and Nanotechnology*, 10(11), 7658–7662.

[21] Patil, P. B., Mali, S. S., Kondalkar, V. V., Mane, R. M., Patil, P. S., Hong, C. K., Bhosale, P. N. (2015). Morphologically controlled electrodeposition of fern shaped Bi2Te3 thin films for photoelectrochemical performance. *Journal of Electroanalytical Chemistry*, 758, 178–190.

[22] Rashid, M. M., Cho, K. H. & Chung, G. -S. (2013). Rapid thermal annealing effects on the microstructure and the thermoelectric properties of electrodeposited Bi2Te3 film. *Applied Surface Science*, 279, 23–30.

[23] Zhou, A., Fu, Q., Zhang, W., Yang, B., Li, J., Ziolkowski, P., Mueller, E. & Xu, D. (2015). Enhancing the thermoelectric properties of the electroplated Bi2Te3 films by tuning the pulse off-to-on ratio. *Electrochimica Acta*, 178, 217–224.

[24] Imam, N. G., Elyamny, S., Aquilanti, G., Pollastri, S., Gigli, L. & Kashyout, A. E. B. (2024). Comprehensive study of nanostructured Bi_2Te_3 thermoelectric materials – insights from synchrotron radiation XRD, XAFS, and XRF techniques. *RSC Advances*, 14(3), 1875–1887.

[25] Humphry-Baker, S. A. & Schuh, C. A. (2014). Grain growth and structural relaxation of nanocrystalline Bi2Te3. *Journal of Applied Physics*,116(15), 153502.

[26] Takashiri, M., Miyazaki, K., Tanaka, S., Kurosaki, J., Nagai, D. & Tsukamoto, H. (2008). Effect of grain size on thermoelectric properties of n-type nanocrystalline bismuth-telluride based thin films. *Journal of Applied Physics*, 104(8), 084302.